A NEW METHOD FOR ENERGY EFFICIENT CEILING FAN BLADE DESIGN: AN AERODYNAMIC APPROACH

Md. Motiur Rahman

ID: 19107034

DEPARTMENT OF MECHANICAL ENGINEERING

COLLEGE OF ENGINEERING AND TECHNOLOGY

IUBAT—INTERNATIONAL UNIVERSITY OF BUSINESS AGRICULTURE AND TECHNOLOGY

SUMMER, 2023

A NEW METHOD FOR ENERGY EFFICIENT CEILING FAN BLADE DESIGN: AN AERODYNAMIC APPROACH

By

Md. Motiur Rahman

ID: 19107034

Program: BSME

A THESIS SUBMITTED IN PARTIAL FULFILMENT OF THE REQUIREMENTS FOR THE DEGREE,

BACHELOR OF SCIENCE IN MECHANICAL ENGINEERING (BSME)

DEPARTMENT OF MECHANICAL ENGINEERING

COLLEGE OF ENGINEERING AND TECHNOLOGY

IUBAT—INTERNATIONAL UNIVERSITY OF BUSINESS AGRICULTURE AND TECHNOLOGY

DECLARATION

This thesis has been prepared after twelve months of research on "A New Method for Energy Efficient Ceiling Fan Blade Design: An Aerodynamic Approach". The thesis is solely for the academic requirement of the course MEC 488 and has not been submitted in part or full elsewhere for any other degree, reward, or any other purpose. we do solemnly declare that all and every right in the copyright of this thesis belongs to IUBAT-International University of Business Agriculture and Technology. Any reproduction or use in any form or by any means whatsoever is prohibited without the written consent of IUBAT.

Md. Motiur Rahman

ID: 19107034

ACKNOWLEDGMENT

First of all, we would like to express our gratitude to our honourable supervisor Dr. Debasish Sarker, Assistant Professor, Department of Mechanical Engineering for his guidance and contribution to our work. Our thesis is the result of his support and effort.

Special thanks to our former supervisor, Assistant Professor, Dr. Sazzad Bin Sharif who is also responsible for this thesis for becoming reality. This thesis topic was selected by him.

We sincerely acknowledge the contributions of Professor and Chair Dr. Dewan Mohammad Nuruzzaman, Associate Professor and Coordinator Dr. A. K. M. Parvez Iqbal, Department of Mechanical Engineering at IUBAT-International University of Business Agriculture and Technology for continuous support to come up with a thesis.

We would like to express our gratitude to the jury for their thoughtful comments which helped us to enrich our thesis project. We also acknowledge the contributions of our faculties at IUBAT-International University of Business Agriculture and Technology for their cooperation, support, and motivation that enabled us to complete our thesis.

We would also like to thank our parents, family members, friends and relatives for their cooperation, affection, and help throughout attending this study. Their support in hard times and motivation to keep doing hard work constantly, helped us a lot to come up with this good work.

Md. Motiur Rahman

ID: 19107034

A NEW METHOD FOR ENERGY EFFICIENT CEILING FAN BLADE DESIGN: AN AERODYNAMIC APPROACH

Candidates

Md. Motiur Rahman
ID: 19107034

Supervisor

Dr. Debasish Sarker
Department of Mechanical Engineering

ABSTRACT

Ceiling fans are commonly used in tropical climates to provide comfort in domestic buildings. Although fan energy consumption is relatively low in comparison to air conditioning, it suffers from some degree of electricity loss which is mainly due to its mechanical inefficiency. This paper illustrates a theoretical and mathematical approach for designing an efficient ceiling fan blade. This new design has been evaluated by computational fluid dynamics (CFD).

TABLE OF CONTENT

LIST OF FIGURES

LIST OF TABLES

LIST OF ABBREVIATIONS

CFD	Computational Fluid Dynamics
RPM	Revolutions Per Minuit
COP	Coefficient of Performance
MRF	Moving Reference Frame
SA	Spalart Allmaras
DM	Design Modeler
DOE	Design of Experiment
NACA	National Advisory Committee for Aeronautics
GOE	Gottingen

LIST OF SYMBOLS

Symbol	Definition	Unit
L	Lift Force	N
C_l	Coefficient of Lift (Infinite Wing)	-
C_L	Coefficient of Lift (Finite Wing)	-
ρ	Density	Kg/m^3
V	Axial Velocity at Blade	m/s
α	Angle of Attack	$Degree$
D	Drag Force	N
C_d	Coefficient of Drag (Infinite Wing)	-
C_D	Coefficient of Drag (Finite Wing)	-
AR	Aspect Ratio	-
e	Span Efficiency Factor	-
$\dot{m}$	Mass Flow Rate	kg/m^3
T	Thrust	N
P_i	Induced Power/ Aerodynamic Power	W
N	Number of Blades	-
C	Chord	m
r	Radial Distance from Centre	m
Ω	Angular Velocity	rad/s
W	Air Inlet Velocity at Blade	m/s
β	Air Inlet Angle at Blade	$Degree$
δ	Pitch Angle	$Degree$
σ	Solidity Ratio	-
ϕ	Hub to Tip Ratio	-
λ	Non-dimensional Induced Velocity	-
C_T	Non-dimensional Thrust	-
C_Q	Non-dimensional Torque	-
Q	Torque	Nm

CHAPTER 1: INTRODUCTION

1.1 Research Background

A ceiling fan is a type of turbo machine that converts the mechanical work done by the rotation of the blades to the kinetic energy of the fluid in this case air. It works similarly to the propeller but it is surrounded by walls and works at a very low angular velocity spectrum compared to the propeller. It is mainly used for cooling purposes.

A ceiling fan is one of the most commonly used electrical appliances used worldwide, especially in tropical regions (Jain et al., 2004). They use a relatively low amount of energy in comparison to the air-conditioning units; they suffer from significant level of electricity loss due to their inefficiencies (Schmidt & Patterson, 2001). The unreasonably high consumption of electrical energy by the conventional ceiling fan is due to high losses at the blades of it, as they are not designed for the optimum aerodynamic performance (Dhurvey et al., 2018). Despite of its low energy efficiency, ceiling fan demand in Bangladesh is around 10 million per year (Ahmed et al., 2016).

1.2 Problem Statement and Significance

Many approaches have been made by previous researchers to improve the efficiency of ceiling fans. However, almost all the research is based on experiment or, computation and doesn't provide any theoretical background for designing more energy-efficient ceiling fan blades.

In this thesis, we are determined to theoretically derive equations which will provide design data for designing energy-efficient fan blades. These equations will be derived from the basic theories of aerodynamics e.g. momentum theory, blade element theory, lifting line theory, and the conservation laws of fluid dynamics e.g. conservation of mass, momentum, and energy.

After deriving the equations, we will check their validity by numerical methods such as Computational Fluid Dynamics (CFD).

1.3 Objectives

- To derive equations for designing ceiling fan blade.
- To apply aerodynamic theories to describe the ceiling fan's aerodynamic properties.
- To validate the equations using numerical methods such as CFD.
- To design energy efficient fan blades using these equations and compare the results with a traditional ceiling fan.

1.4 Organization of the Report

This thesis is organized into five chapters. The first chapter is about the research background and objective of this study. In Chapter 2, an elaborate literature review is presented about different studies in the research area of the ceiling fan. Chapter 3 contains theoretical derivation for the design procedure of a ceiling fan and a full setup procedure for numerical solution. Chapter 4 includes numerical results and discussions of obtained results respectively. The conclusion of this research work is drawn in chapter 5 along with constructive recommendations and potential possibilities for further study.

1.5 Limitations of the Report

- This report doesn’t contain any experimental data.
- It is highly based on theoretical and numerical results.

CHAPTER 2: LITERATURE REVIEW

2.1 Literature Survey

Through a series of tests, the flow field of a ceiling fan in an empty room. Smoke visualization allowed for the identification of several flow zones within the space. A comparison of fan blades with and without winglets was performed to improve the air circulation inside the space. The goal was to stop the blade tip vortices from creating any induced flow at the tips of the fan blades. With the same amount of power, the downward air velocity was boosted by 13% thanks to spikes and winglets (Jain et al., 2004).

Schmidt and Patterson experimentally compared the effectiveness of several fan blade designs. A four-bladed prototype fan with a high angle of attack was created, and it achieved the rated airflow at 140 revolutions per minute (rpm), as opposed to the normal ceiling fan's 270 rpm. It was possible to create an aerodynamically effective fan blade by combining different design elements, including blade profile, geometric twist, and taper ratio. According to the study's findings, the new ceiling fan design can reduce power consumption in comparison to traditional ceiling fans by a factor of up to three (Schmidt and Patterson, 2001).

Dhurvey et al. established a complete analysis of ceiling fan for four different blade materials. Structural analysis and aerodynamics analysis is done using ANSYS (CFX) 14.0 Software. COP analysis is done using MATLAB R2015a Program and power consumption analysis is also presented. The deflection of all blade at their tip are maximum, in which PVC blade undergoes more deflection than blade made of other material though PVC blade has maximum deflection but is in limit, the stresses generated in it is less than others. By reducing the weight of blades, the power needed for operating the ceiling fan will be decreased (Dhurvey et al., 2018).

Mahlia et al. focused on creating a new ceiling fan blade configuration capable of lowering the power consumption of the traditional blade, resulting in a fan with improved efficiency. This blade adopts a thin airfoil shape and the performance of the fan was evaluated through experimental and computational techniques. It was observed that the COP of the newly designed ceiling fan is 2.85 while the COP of the conventional fan is 2.74 (Mahlia et al., 2011).

Rajapakshe et al. identified the flow patterns around the ceiling fan and thereby determine the effective operating parameters experimentally and numerically. For numerical modeling, computational fluid dynamics (CFD) was used with the moving reference frame (MRF) technique and Spalart-Allmaras (SA) turbulence model (Rajapakshe et al., 2015).

Afaq et al. experimentally and numerically studied ceiling fan performance to produce more efficient ceiling fan blades. This paper uses the Design of Experiment (DoE) to achieve a new blade design with improved efficiency. It achieved improvements of 21% in RAD, 22% in power consumption, and 54% in SV are attained with the proposed modification (Afaq et al., 2017).

2.2 Summary

The above discussion gives an idea about the ceiling fan design process at the research level. Previous researcher doesn't apply aerodynamic theories to improve the fan blade design process. In this thesis we attempted to apply aerodynamic theories to improve fan blade design process.

CHAPTER 3: AERODYNAMIC THEORIES

3.1 Introduction

Understanding the motion of air around an object (often called a flow field) enables the calculation of forces and moments acting on the object. In many aerodynamic problems, the forces of interest are the fundamental forces of flight: lift, drag, thrust, and weight. Lift and drag are aerodynamic forces, i.e., due to airflow over a solid body. These quantities' calculations are often founded upon the assumption that the flow field behaves as a continuum. Continuum flow fields are characterized by properties such as flow velocity, pressure, density, and temperature, which may be functions of position and time. These properties may be directly or indirectly measured in aerodynamics experiments or calculated starting with the equations for the conservation of mass, momentum, and energy in air flows. Density, flow velocity, and an additional property, viscosity, are used to classify flow fields.

The assumption of a fluid continuum allows problems in aerodynamics to be solved using fluid dynamics conservation laws. Three conservation principles are used:

- **Conservation of Mass:** Conservation of mass requires that mass is neither created nor destroyed within a flow; the mathematical formulation of this principle is known as the mass continuity equation.

$$\dot{m} = \rho A V \tag{1}$$

Differential Form,

$$\nabla \cdot (\rho \mathbf{V}) = 0 \tag{2}$$

- **Conservation of Momentum:** The mathematical formulation of this principle can be considered an application of Newton's Second Law. Momentum within a flow is only changed by external forces, which may include surface forces, such as viscous (frictional), and body forces, such as weight. The momentum conservation principle may be expressed as either a vector equation or separated into a set of three scalar equations (x,y,z components).

$$\rho \frac{Du}{Dt} = -\frac{\partial p}{\partial x} \tag{3}$$

$$\rho \frac{Dv}{Dt} = -\frac{\partial p}{\partial y} \tag{4}$$

$$\rho \frac{Dw}{Dt} = -\frac{\partial p}{\partial z} \tag{5}$$

- **Conservation of Energy:** The energy conservation equation states that energy is neither created nor destroyed within a flow and that any addition or subtraction of energy to a volume in the flow is caused by heat transfer, or by work into and out of the region of interest.

$$\rho \frac{D(e + V^2/2)}{Dt} = \rho \dot{q} - \nabla \cdot (\rho \mathbf{V}) \tag{6}$$

Where,

$$\frac{D}{Dt} = \frac{\partial}{\partial t} + (\mathbf{V} \cdot \nabla)$$

that is, the local derivative plus the convective derivative. In the above equations u, v and w are the velocities in the Cartesian directions x, y and z respectively; ρ is the fluid density; p is the pressure; $\mathbf{V}$ is the velocity of the fluid element; e is the internal kinetic energy per unit volume; $\dot{q}$ is the volumetric rate of heat addition and t is time

3.2 Aerodynamic Forces

Many forces act on bodies submerged in air, these are called aerodynamic forces e.g. lift, drag, thrust, etc. Among these forces, we will focus on lift and drag.

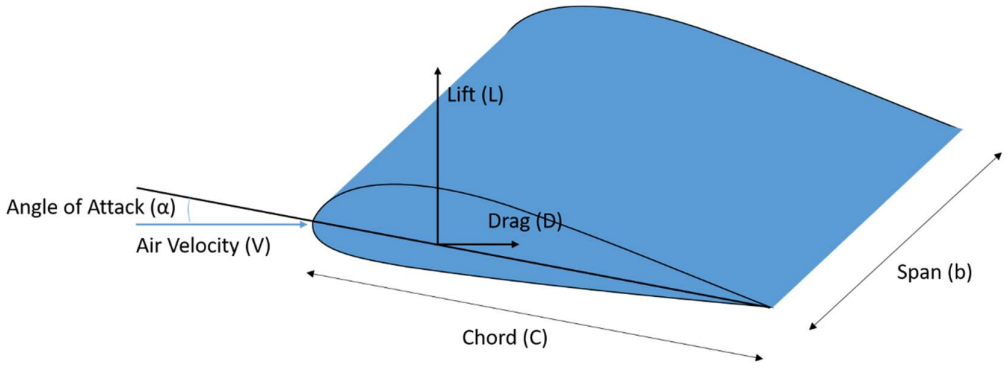

Figure 3.1: Aerodynamic Forces Acting on a Wing

3.2.1 Lift Force

A fluid flowing around an object exerts a force on it. Lift is the component of this force that is perpendicular to the oncoming flow direction (NASA Glenn Research Center, 2022).

Lift,

$$L = \frac{1}{2} C_l \rho A V^2 \tag{7}$$

Or,

$$L = \frac{1}{2} C_l \rho C b V^2 \tag{8}$$

Here, L is lift force on the blade; C_l is the coefficient of lift; ρ is the density of the fluid; A is the area of the blade C times b, where C is the chord and b is the span; V is the velocity of incoming air; and α is the angle of attack.

3.2.2 Drag Force

Aerodynamic drag force is defined as the force that is faced by the vehicle as it moves through the air (Sheng, 2019).

Drag,

$$D = \frac{1}{2} C_d \rho A V^2 \tag{9}$$

Or,

$$D = \frac{1}{2} C_d \rho C b V^2 \tag{10}$$

Here, D is drag force on the blade; C_d is the coefficient of drag; ρ is the density of the fluid; A is the area of the blade C times b, where C is the chord and b is the span; V is the velocity of incoming air; and α is the angle of attack.

3.2.3 Coefficient of Lift

The coefficient of lift is a non-dimensional number associated with lift force. It is an experimental value, and it is a function of the angle of attack for a given shape.

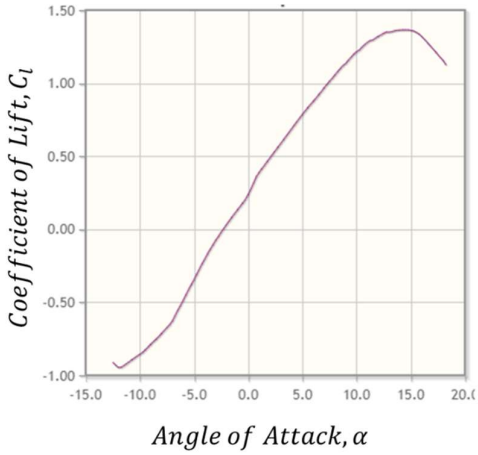

Figure 3.2: Lift Coefficient vs. Angle of Attack

Coefficient of Lift,

$$C_l = \frac{L}{\frac{1}{2}\rho A V^2} \tag{11}$$

Or,

$$C_l = \frac{L}{\frac{1}{2}\rho C b V^2} \tag{12}$$

3.2.4 Coefficient of Drag

The coefficient of drag is a non-dimensional number associated with drag force. It is an experimental value, and it is a function of the angle of attack for a given shape.

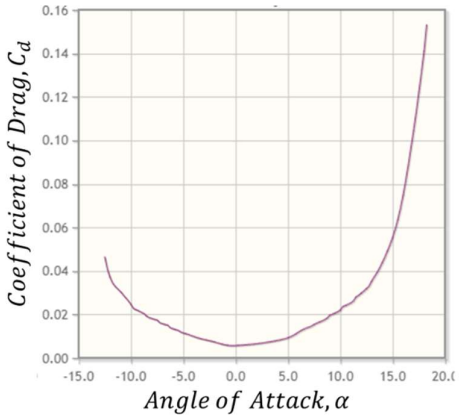

Figure 3.3: Drag Coefficient vs. Angle of Attack

Coefficient of Drag**,**

$$C_d = \frac{D}{\frac{1}{2}\rho A V^2} \tag{13}$$

Or,

$$C_d = \frac{D}{\frac{1}{2}\rho C b V^2} \tag{14}$$

3.2.5 Lifting Line Theory

Previously we discussed the lift and drag forces and the coefficients of an infinite wing. But most of the real-life wings have a finite wing span. In real cases, the values of lift predicted by the theory were not accurate. Ludwig Prandtl and his colleagues were trying to solve this issue in Göttingen, Germany, during the period 1911 – 1918 [12]. He stated that the tips of the wing create vortices which cause downwash at the tip of the wing and result in induced drag which reduces lift. Then he came up with a solution to predict the actual lift and drag of a finite wing which is called Prandtl Lifting Line Theory.

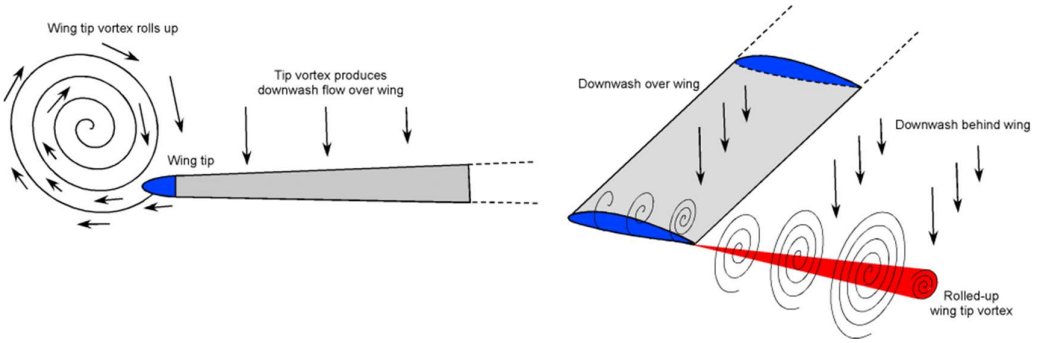

Figure 3.4: Induced Velocity and Downwash

The Lifting Line Theory introduces two new coefficients C_L associated with lift and C_D associated with drag.

Here,

$$C_L(Finite\ Wing) \neq C_l(Infinite\ Wing)$$

$$C_D(Finite\ Wing) \neq C_d(Infinite\ Wing)$$

Where the value C_L is less than C_l and the value of C_D is higher than C_d.

Coefficient of Lift of Finite Wing,

$$C_L = a(\alpha - \alpha_{L=0}) \tag{15}$$

$$a = \frac{a_0}{1 + \frac{a_0}{\pi AR}(1+\tau)} \tag{16}$$

$$a_0 = \frac{dC_l}{d\alpha} \tag{17}$$

Here, C_L is the coefficient of lift of a finite wing; C_l is the coefficient of lift of infinite wing; α is the geometric angle of attack; $\alpha_{L=0}$ is the zero lift angle; AR is the aspect ratio; and $\tau\ is\ a\ function\ of\ Fourier\ Transform.$

Coefficient of Drag of Finite Wing,

$$C_D = C_d + C_{Di} \tag{18}$$

$$C_{Di} = \frac{C_L^2}{\pi AR}(1+\delta) \tag{19}$$

$$C_D = C_d + \frac{C_L^2}{\pi AR}(1+\delta) \tag{20}$$

$$e = \frac{1}{1+\delta} \tag{21}$$

Substituting equation 21 into equation 20,

$$C_D = C_d + \frac{C_L^2}{\pi e AR} \tag{22}$$

Here, C_D is the coefficient of drag of a finite wing; C_d is the coefficient of drag of infinite wing; C_{Di} is the coefficient of induced drag; AR is the aspect ratio; and e is the span efficiency factor.

3.2.6 The Momentum Theory

In fluid dynamics, momentum theory or disk actuator theory is a theory describing a mathematical model of an ideal actuator disk, such as a propeller or helicopter rotor, by W.J.M. Rankine (Sheng et al., 2019) Alfred George Greenhill and Robert Edmund Froude (Froude and William, 1865).

The rotor is modelled as an infinitely thin disc, inducing a constant velocity along the axis of rotation. The basic state of a helicopter is hovering. This disc creates a flow around the rotor. Under certain mathematical premises of the fluid, there can be extracted a mathematical connection between power, radius of the rotor, torque, and induced velocity.

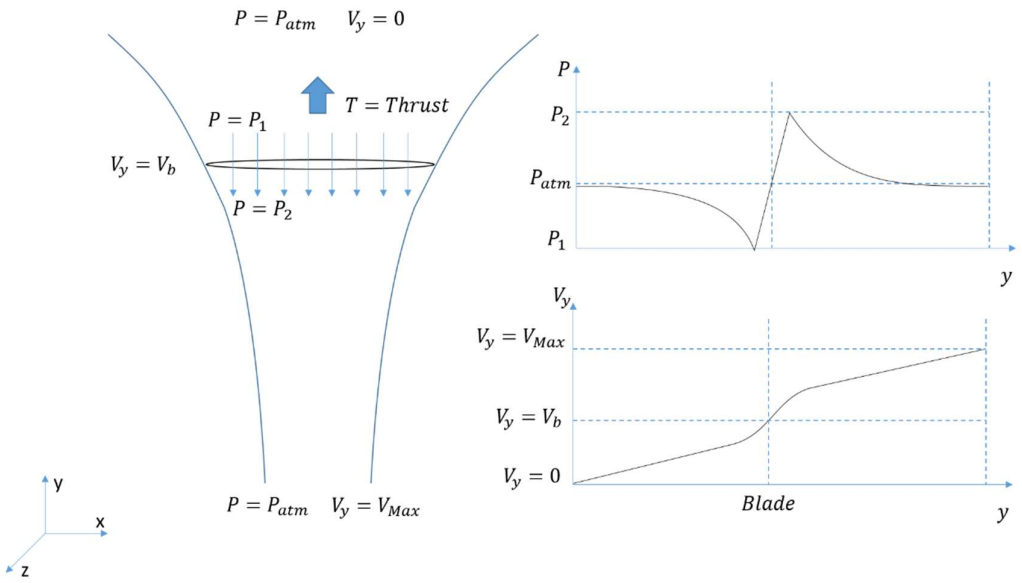

Figure 3.5: Flow Field, Pressure, and Velocity Profile of a Propeller

Assumptions:

1. The rotor blade is considered as an actuator disk.
2. Uniform inflow at the rotor.

From the Conservation of Mass,

Mass Flow Rate,

$$\dot{m} = \rho A V_b \tag{1}$$

Here, $\dot{m}$ is the mass flow rate; A is the area of the actuator disk; and V_b is the vertical component of induced velocity of air at the actuator disk.

From the Conservation of Momentum,

Thrust,

$$T = \dot{m}\Delta V_y$$

$$T = \dot{m}(V_{Max} - 0)$$

$$T = \dot{m} V_{Max}$$

$$T = \rho A V_b V_{Max} \tag{23}$$

Here, T is the thrust produced by the propeller; ΔV_y is the change in velocity; and V_{Max} is the velocity of air at the far downstream where velocity tends to maximize.

From the Conservation of Energy,

Change in kinetic energy per second,

$$\Delta \dot{K} = \frac{1}{2} \dot{m} V_{Max}^2$$

$$\Delta \dot{K} = \frac{1}{2} \rho A V_b V_{Max}^2 \tag{24}$$

Induced Power at the Disk,

$$Power = Force(Thrust) \times Velocity\ at\ Disk$$

$$P_i = T V_b \tag{25}$$

We know, equation 25 is equal to equation 24,

$$P_i = \Delta \dot{K}$$

$$T V_b = \frac{1}{2} \rho A V_b V_{Max}^2$$

$$V_{Max} = 2 V_b$$

Thrust,

$$T = \rho A V_b V_{Max}$$

$$T = \rho A V_b (2 V_b)$$

$$T = 2 \rho A V_b^2 \tag{26}$$

3.2.7 Blade Element Theory

Blade element theory (BET) is a mathematical process originally designed by William Froude (Froude and Robert, 1889) to determine the behaviour of propellers. It involves breaking a blade down into several small parts and then determining the forces on each of these small blade elements. These forces are then integrated along the entire blade and over one rotor revolution to obtain the forces and moments produced by the entire propeller or rotor. One of the key difficulties lies in modelling the induced velocity on the rotor disk. Because of this, the blade element theory is often combined with momentum theory to provide additional relationships necessary to describe the induced velocity on the rotor disk, producing blade element momentum theory.

Blade element theory is based on dividing the blade up into a large number of elementary strips, as seen in Figure 2.6. Each of these elementary strips can then be regarded as an aerofoil subject to a resultant incident velocity W.

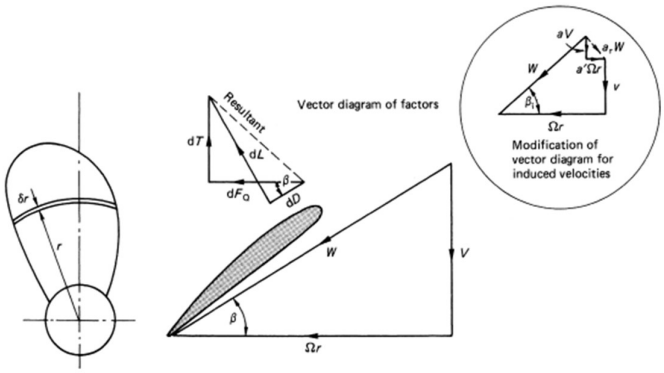

Figure 3.6: Propeller Blade Section for BET
("Marine Propellers and Propulsion," 2012, pp. 172)

The resultant incident velocity was considered to comprise an axial velocity V together with a rotational velocity Ur, which clearly varies linearly up the blade. In the normal working condition, the advance angle b is less than the blade pitch angle q at the section, and hence gives rise to the section having an angle of incidence a. The section will, therefore, experience lift and drag forces from the combination of this incidence angle and the section zero lift angle, from which one can deduce that, for a given section geometry, the elemental thrust and torques are given by

Elemental Thrust,

$$dT = \frac{1}{2}\rho NCW^2(C_L cos\beta - C_D sin\beta)dr \quad (27)$$

Elemental Torque,

$$dQ = \frac{1}{2}\rho NCW^2(C_L sin\beta + C_D cos\beta)rdr \quad (28)$$

where N and C are the number of blades and the chord length of the section respectively.

CHAPTER 4: METHODOLOGY

4.1 Introduction

In this chapter, we will give a detailed description of our CFD setup using Ansys Fluent 2023 R2 Student Version, how we can use aerodynamic theories to improve ceiling fan performance, and lastly testing our new fan blade model in our CFD setup.

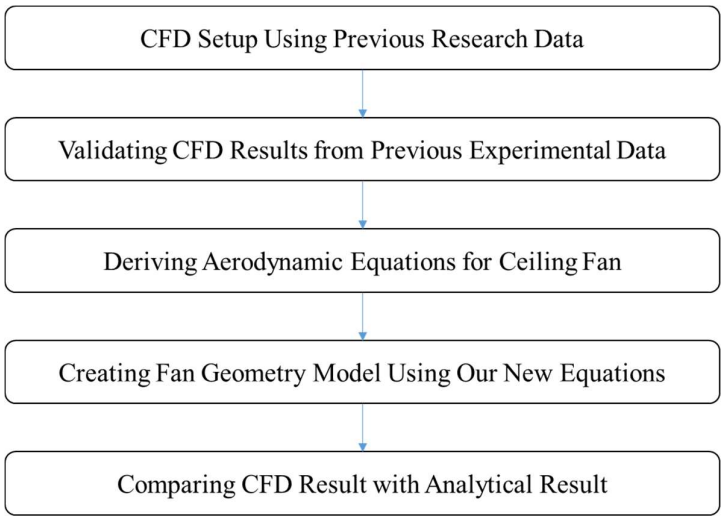

Figure 4.1: Operation Process

4.2 CFD Setup

In this section, we will create a CFD model setup using Ansys Fluent 2023 R2 Student Version and related software applications using previous research data (Afaq et al., 2017).

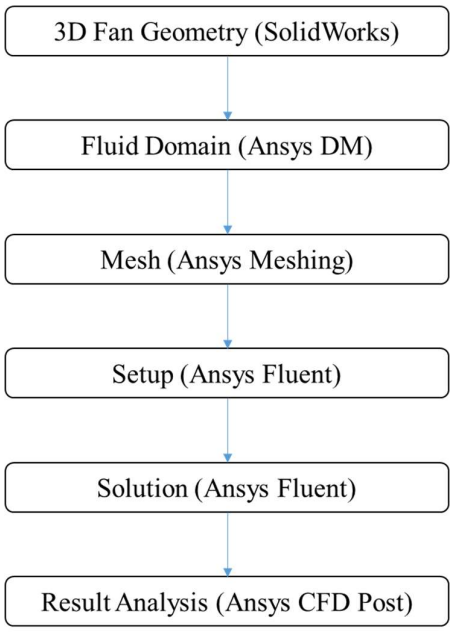

Figure 4.2: CFD Setup Process

4.2.1 Description of Fan Geometry

Figure 3.3 shows the conventional configuration of a ceiling fan used as the basis for the studies. A ceiling fan consists of two major parts: hub and blades. The central rotating part to which the blades are attached is called the fan hub. Its purpose is to house an electric motor. The blade section that is attached to the hub is called the blade root, whereas the outermost end is called the blade tip. The diameter of the ceiling fan used in the research for benchmark purposes was 1.42 m, based on the circular area swept by the ceiling fan during operation. The angle between the horizontal plane containing the root chord and the plane midway between the upper and lower surfaces of the blade is known as the rake angle, which helps to spread the air. The bend angle is defined as the angle between the two surfaces of the blade. The function of this angle is to push more air downwards in the room, as shown in Figure 3.3. The leading edge is part of the blade that first contacts the air; alternatively, it is the foremost edge of an airfoil section. The trailing edge of the blade is its rear edge.

The baseline geometry widely used by various manufacturers was selected to get the coordinates of the blade profile. The length of the fan blade was 0.57 m, the chord length at the root and tip being 0.16 m and 0.12 m respectively. Aluminum was used to make the blade with a thickness of 0.001 m. The diameter of the fan hub was 0.26

m and the total diameter of the fan including the hub was 1.42 m. The selected fan consisted of three aluminum blades with a bend angle of 11.8° and a rake angle of 5°. The bend position at the root and tip chord was 63% and 17% of the chord length respectively. All three blades were 120° apart from each other. The experimentally measured fan dimensions are shown in Table 3.1.

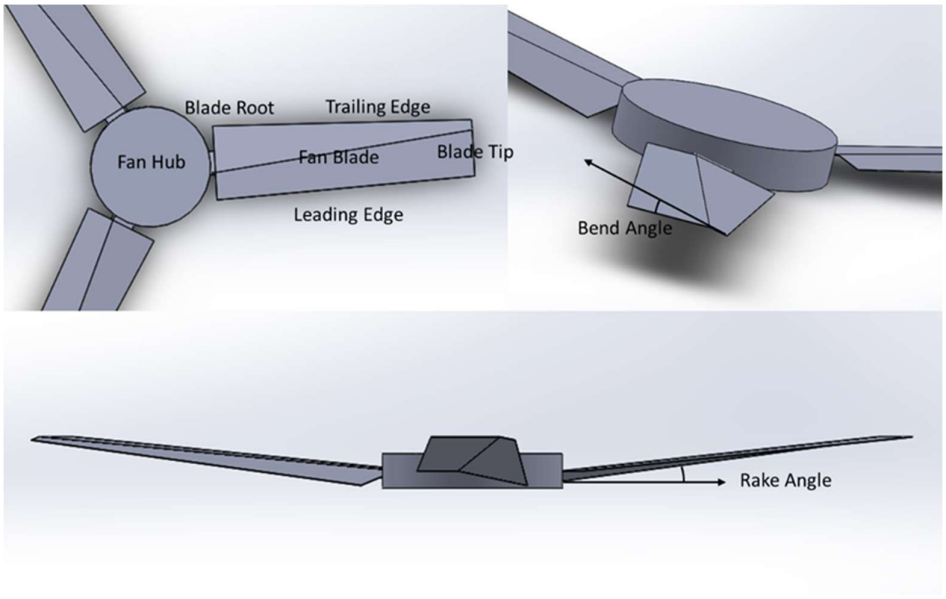

Figure 4.3: Fan Blade Geometry

Table 4.1: Geometric dimensions of ceiling fan under study

Geometric Attribute	Dimension
Fan Hub Diameter	0.26 m
Fan Blade Length	0.57 m
Fan Diameter	1.42 m
Fan Blade Thickness	0.001 m
Fan Blade Material	Aluminum
Fan Blade Bend Angle	11.8^0
Fan Blade Rake Angle	5^0
Fan Blade Root Chord	0.16 m
Fan Blade Tip Chord	0.12 m

4.2.2 Computational Modelling

The ceiling fan geometry includes three blades and a hub in a rotatory disk. The coordinates of geometry were taken from the original model and reproduced in SOLIDWORKS®. For simplicity, the rivets and connectors were removed in the computational domain because they have negligible effect on the flow. Unstructured tetrahedral mesh elements were used to mesh the flow field of rotating domain (fan disk) and stationary domain (test room). To improve the quality or accuracy of the simulation, a matching grid at the interface of two grid blocks was generated.

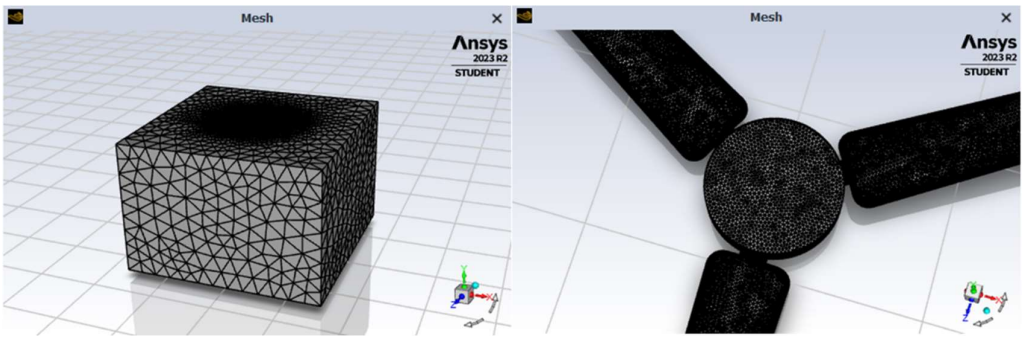

Figure 4.4: Computational Domain of Fan and Room

A grid independence study was carried out by developing grids of three different sizes, as shown in Figure 3.5. The purpose of grid independence study is to achieve a set of grid points for which the solution and the flow physics of the computational case do not further change if the level of mesh refinement is increased. The grid with the best results in terms of flow profile and computational efficiency was selected for further analysis. For this purpose, three meshes were generated, with cell numbers of 0.75, 0.85 and 1 million in coarse, medium and fine grid respectively. All three sets of mesh were computationally solved using the S-A turbulence model. The computational domain has a fine grid near the ceiling fan and a coarse one further away. The grid with 0.85 million cells was selected based on the trade-off between accuracy and computation speed.

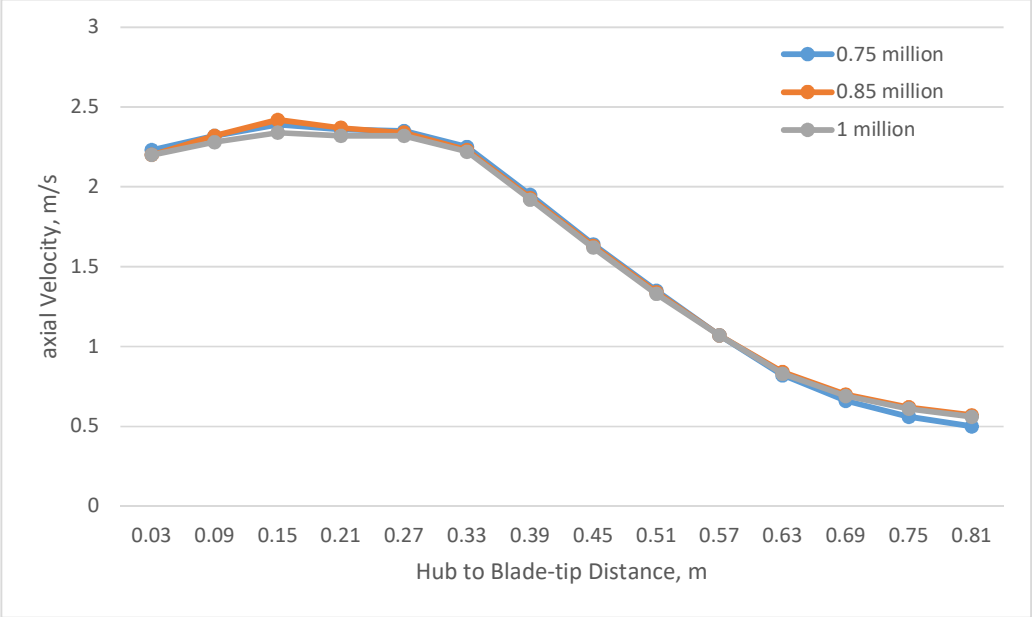

Figure 4.5: Grid Independence Study

After grid selection, a turbulence model sensitivity study was also carried out to compare k-Omega, k-Epsilon and S-A models with experimental data. Results in Figure 3.6 clearly show that the S-A turbulence model best agrees with experimental values.

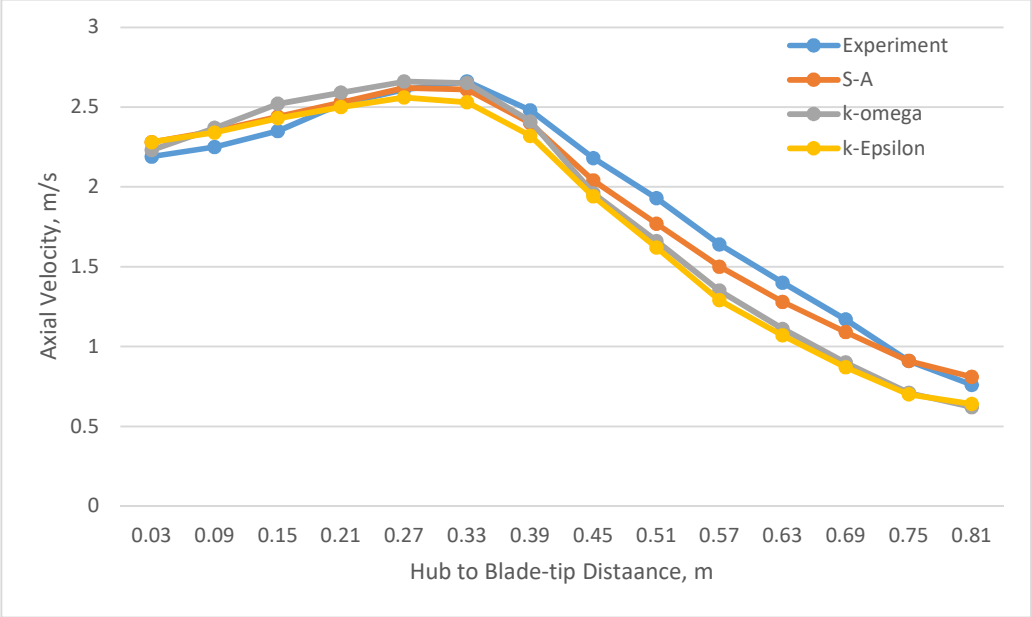

Figure 4.6: Comparison of Turbulence Models

For the selection of turbulence model, all the computations were performed using the finite volume code Fluent® with a steady-RANS approach. No-slip velocity or

adiabatic wall boundary condition was enforced at the blade surfaces, fan hub and room walls. The static pressure was set to 101325 Pa, and the fan speed was set to 300 rpm. The turbulence dissipation rate and momentum discretization scheme were determined through a second-order upwind scheme. SIMPLE algorithm [14] was used to couple pressure and velocity. A coupled solver was used with an implicit formulation to solve discretized equations and the Courant number was set to 5 for fast convergence.

4.2.3 Validation Study

A comparison of computational and experimental velocity profiles at 1.5 m below the ceiling fan is shown in Figure 3.7. Comparison of computational fluid dynamics (CFD) simulations with laboratory tests shows a reasonable fit within 5% bounds of the air velocity behavior.

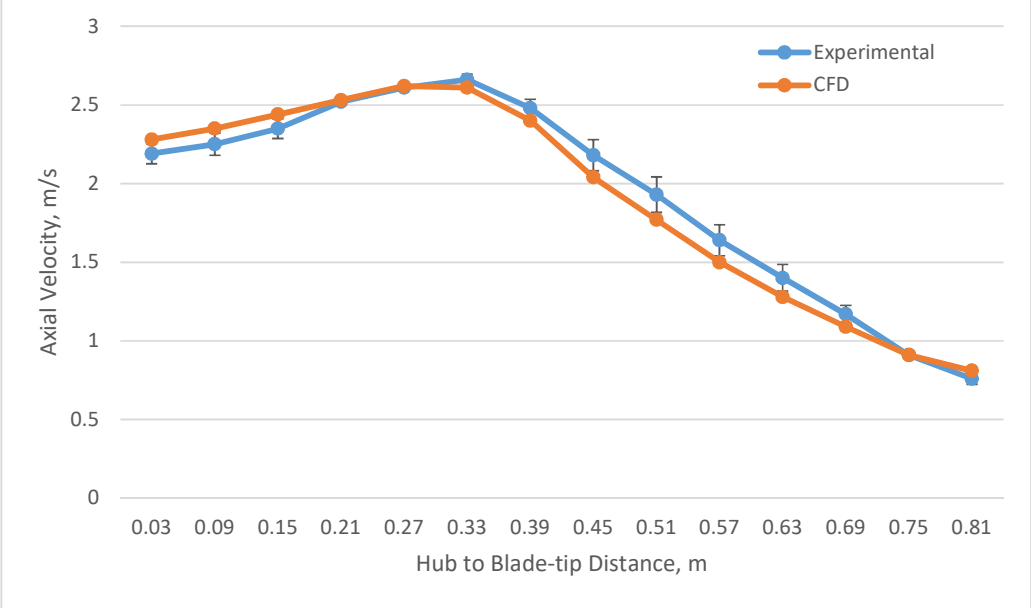

Figure 4.7: Comparison of Experimental and CFD axial Velocity at 300 RPM

4.3 Application of Aerodynamic Theories in Ceiling Fan Design

4.3.1 Applying the Momentum Theory to Ceiling Fan

The flow field of the ceiling fan is quite similar to the flow field of the propeller.

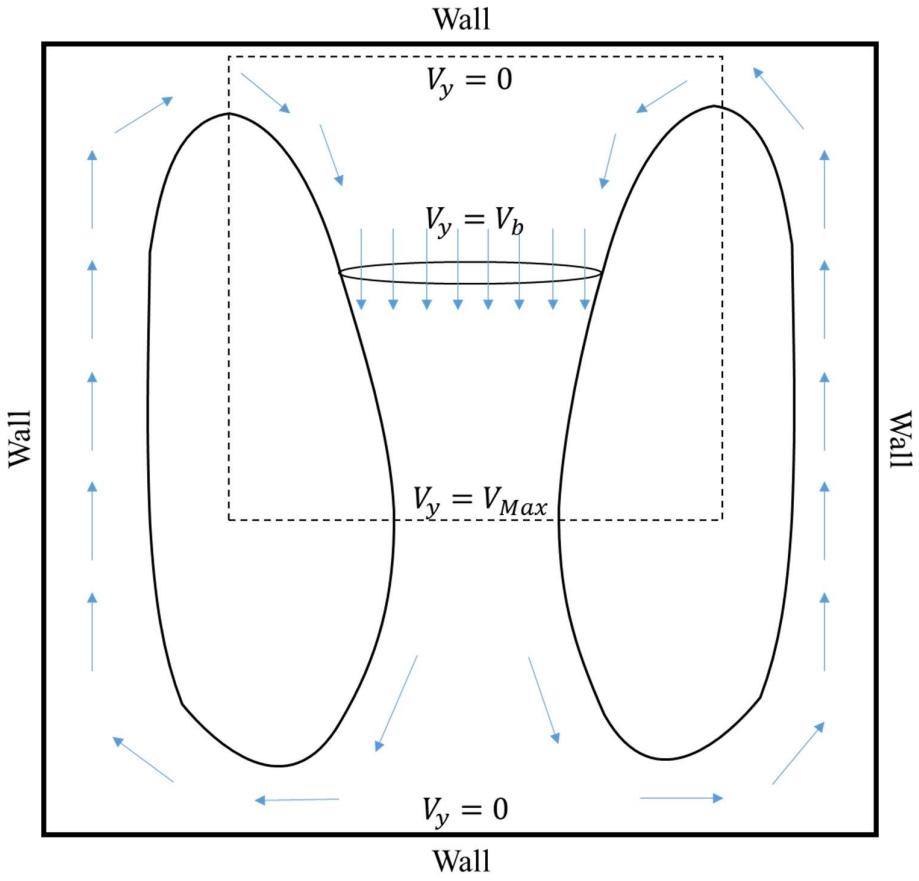

Figure 4.8: A Flow Field of Ceiling Fan

The above figure shows the flow field of the air through a ceiling fan. If we take a control volume around the fan region so that the flow field matches with the flow field of the momentum theory, then we can use momentum theory to design our ceiling fan blade. By looking closely into the control volume we can assume that the flow field created by a ceiling fan is similar to the flow field from momentum theory. So that, we might be able to use momentum theory in our ceiling fan design.

4.3.2 Theoretical Derivation

Assumptions:

1. Uniform Air Inflow
2. Constant chord throughout the entire blade
3. Fixed angle of attack with the resultant flow
4. Constant coefficient of lift throughout the entire blade
5. Flow is incompressible
6. Flow is steady

From Blade Element Theory,

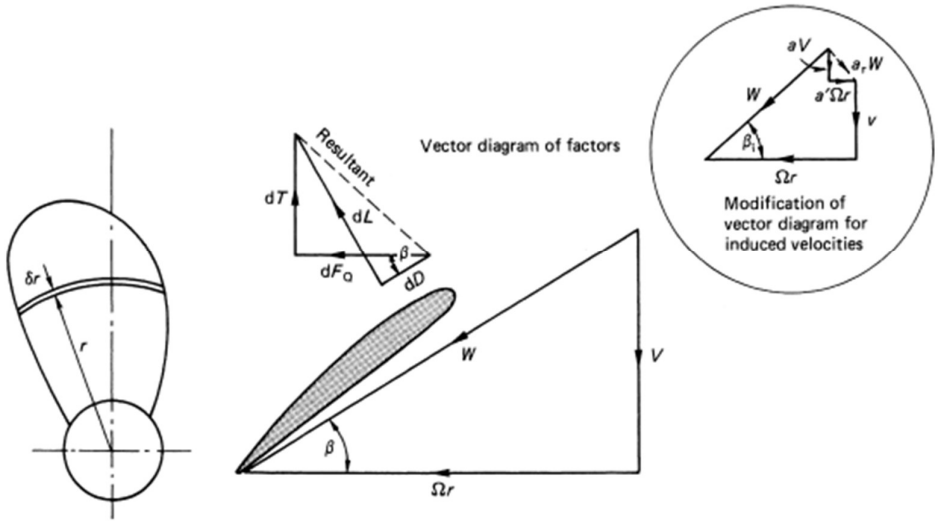

Figure 4.9: Blade Element Theory Implementation
("Marine Propellers and Propulsion,"2012, pp. 172)

Elemental Thrust,

$$dT = \frac{1}{2}\rho NCW^2(C_L cos\beta - C_D sin\beta)dr \tag{27}$$

Applying trigonometry in equation 27,

$$dT = \frac{1}{2}\rho NC\left(C_L \Omega r\sqrt{(\Omega r)^2 + V^2} - C_D V\sqrt{(\Omega r)^2 + V^2}\right)dr \tag{29}$$

Elemental Torque,

$$dQ = \frac{1}{2}\rho NCW^2(C_L sin\beta + C_D cos\beta)rdr \tag{28}$$

Applying trigonometry in equation 28,

$$dQ = \frac{1}{2}\rho NC\left(C_L V\sqrt{(\Omega r)^2 + V^2} + C_D \Omega r\sqrt{(\Omega r)^2 + V^2}\right)rdr \tag{30}$$

Thrust,

Integrating equation 29,

$$T = \int_0^R \frac{1}{2}\rho NC\left(C_L \Omega r\sqrt{(\Omega \mathrm{r})^2 + V^2} - C_D V\sqrt{(\Omega r)^2 + V^2}\right)dr$$

$$T = \frac{1}{2}\rho NC\int_0^R \left(C_L \Omega r\sqrt{(\Omega \mathrm{r})^2 + V^2} - C_D V\sqrt{(\Omega r)^2 + V^2}\right)dr$$

$$T = \frac{1}{6}\rho NCC_L\Omega^2 R^3 - \frac{1}{4}\rho NCC_D V\Omega R^2$$

Dividing both sides by, $\rho NCR(\Omega R)^2$

$$\frac{T}{\rho NCR(\Omega R)^2} = \frac{1}{6}C_L - \frac{1}{4}C_D\frac{V}{\Omega R} \tag{31}$$

Let,

$$\lambda = \frac{V}{\Omega R} \tag{32}$$

$$C_T = \frac{T}{\rho NCR(\Omega R)^2} \tag{33}$$

Substituting λ and C_T in equation 31,

$$C_T = \frac{1}{6}C_L - \frac{1}{4}C_D\lambda \tag{34}$$

Implementing the value of 'T' from the momentum theory in equation 31,

$$\frac{2\rho AV^2}{\rho NCR(\Omega R)^2} = \frac{1}{6}C_L - \frac{1}{4}C_D\lambda$$

$$\frac{2\rho\pi(R^2 - r_{hub})V^2}{\rho NCR(\Omega R)^2} = \frac{1}{6}C_L - \frac{1}{4}C_D\lambda$$

$$\frac{2\pi R^2V^2}{NCR(\Omega R)^2} - \frac{2\pi R^2V^2}{NCR(\Omega R)^2}\frac{r_{hub}^2}{R^2} = \frac{1}{6}C_L - \frac{1}{4}C_D\lambda \tag{35}$$

Let,

$$\sigma = Solidity\ Ratio = \frac{NCR}{\pi R^2} \tag{36}$$

$$\phi = Hub\ to\ Tip\ Ratio = \frac{r_{hub}}{R} \tag{37}$$

So,

$$\frac{2\lambda^2}{\sigma} - \frac{2\lambda^2}{\sigma}\phi^2 = \frac{1}{6}C_L - \frac{1}{4}C_D\lambda$$

$$\frac{2}{\sigma}(1-\phi^2)\lambda^2 = \frac{1}{6}C_L - \frac{1}{4}C_D\lambda$$

$$24(1-\phi^2)\lambda^2 + 3C_D\sigma\lambda - 2C_L\sigma = 0 \tag{38}$$

Torque,

Integrating equation 30,

$$Q = \frac{1}{2}\rho NC\int_0^R \left(C_L V\sqrt{(\Omega r)^2 + V^2} + C_D\Omega r\sqrt{(\Omega r)^2 + V^2}\right) rdr$$

$$Q = \frac{1}{6}\rho NCC_L V\Omega R^2 + \frac{1}{8}\rho NCC_D\Omega^2R^4$$

$$\frac{Q}{\rho NC\Omega^2R^4} = \frac{1}{6}C_L\lambda + \frac{1}{8}C_D \tag{39}$$

Let,

$$C_Q = \frac{Q}{\rho N C \Omega^2 R^4} \tag{40}$$

Substituting C_Q in equation 39,

$$C_Q = \frac{1}{6} C_L \lambda + \frac{1}{8} C_D \tag{40}$$

Therefore,

$$\sigma = \frac{\pi R}{NC}$$

$$\phi = \frac{r_{hub}}{R}$$

$$24(1 - \phi^2)\lambda^2 + 3C_D \sigma \lambda - 2C_L \sigma = 0$$

$$C_T = \frac{1}{6} C_L - \frac{1}{4} C_D \lambda$$

$$C_Q = \frac{1}{6} C_L \lambda + \frac{1}{8} C_D$$

$$V = \lambda \Omega R \tag{41}$$

$$T = C_T \rho N C \Omega^2 R^3 \tag{42}$$

$$Q = C_Q \rho N C \Omega^2 R^4 \tag{43}$$

Efficiency,

$$\eta = \frac{Aerodynamic\ Power\ Output}{Power\ Requir\ to\ Rotate\ Fan}$$

$$\eta = \frac{TV}{Q\Omega} \tag{44}$$

$$\eta = \frac{C_T \lambda}{C_Q} \tag{45}$$

4.4 Evaluation of Theory

We have modelled six individual fan blades and simulated them using our verified CFD setup. For the first three cases, we used NACA 2410 aerofoil for different numbers of blades, but with the same chord. In the second three cases, we used GOE 227 aerofoil for different chords, but with the same number of blades.

Sample Case:

Table 4.2: Aerofoil Characteristics

Aerofoil	NACA 2410
Optimal Angel of Attack, α	4.5°
Coefficient of Lift, C_l	0.7383
Coefficient of Drag, C_d	0.00767
Zero Lift Angle, $\alpha_{L=0}$	-2.25
$a_0 = \frac{dC_l}{d\alpha}$	$6.0766\ rad^{-1}$

Table 4.3: Geometric Attributes

Chord, C	0.1 m
Number of Blades, N	3
Fan Hub Diameter, r_{hub}	0.13 m
Fan Blade Span, b	0.56 m
Fan Radius, R	0.7 m

Table 4.4: Fan Blade Aerodynamic Parameters

AR	5.6
τ	0.09
a	$0.077\ degree^{-1}$
C_L	0.51975
C_D	0.0244

Calculating Thrust, Torque and Axial Velocity at Blade

Solidity Ratio:

$$\sigma = \frac{\pi R}{NC}$$

$$\sigma = 0.136418204$$

Hub to Tip Ratio:

$$\phi = \frac{r_{hu}}{R}$$

$$\phi = 0.185$$

Axial Velocity at Blade:

$$24(1-\phi^2)\lambda^2 + 3C_D\sigma\lambda - 2C_L\sigma = 0$$

$$\lambda = \frac{-3C_D \pm \sqrt{(3C_D)^2 + 192(1-\phi^2)C_L\sigma}}{48(1-\phi^2)}$$

$$\lambda = 0.07823$$

$$\lambda = -0.07756\ (Not\ accepted)$$

$$V = \Omega R$$

$$V = 1.1435\ \text{m/s}$$

Thrust:

$$C_T = \frac{1}{6} C_L - \frac{1}{4} C_D \lambda$$

$$C_T = 0.0797$$

$$T = C_T \rho N C \Omega^2 R^3$$

$$T = 4.423 \text{ N}$$

Torque:

$$C_Q = \frac{1}{6} C_L \lambda + \frac{1}{8} C_D$$

$$C_Q = 0.00981$$

$$Q = C_Q \rho N C \Omega^2 R^4$$

$$Q = 0.38\ Nm$$

Blade is designed through applying various pitch angle at various section of the blade. Pitch angle is calculated using the following formula:

Pitch Angle:

$$\delta = \beta + \alpha$$

Where, β is the angel of incoming air and AOA is the angel of attack.

$$\tan \beta = \frac{V}{\Omega r}$$

$$\beta = \tan^{-1} \frac{V}{\Omega r}$$

$$\delta = \tan^{-1} \left(\frac{V}{\Omega r} \right) + \alpha$$

Table 4.5: Blade Design Parameters

Distance from Hub Center, r	Pitch Angle (Degree)
0.14 m	25.66101896
0.28 m	15.45392917
0.42 m	11.85228856
0.56 m	10.02747156
0.70 m	8.926916589

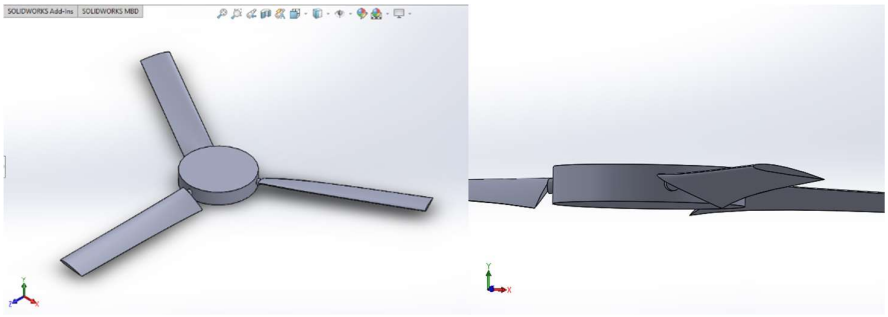

Figure 4.10: 3D Geometry of Sampler Case

Table 4.6: CFD Results of Sample Case

Thrust	4.449 N
Torque	0.447 Nm
Average Velocity at Blade	1.1 ms^{-1}

Table 4.7: Comparison between CFD and Analytical Results

Parameters	Analytical Result	CFD Result	Error
Thrust (N)	4.764	4.449	7%
Velocity at Blade (ms^{-1})	1.14	1.1	4%

From the above comparison, we can say that our equation can predict more than 90% accurate results. For more convenience, we have made five more models and tested them using Ansys Fluent 2023 R2 Student Version.

Table 4.8: Analytical and CFD Result Compression for all 6 cases

Aerofoil	Chord (m)	No of Blade	Analytical Thrust (N)	CFD Thrust (N)	Error
NACA 2410	0.1	2	3.179	3.276	3%
	0.1	3	4.764	4.449	7%
	0.1	6	9.506	8.713	9%
GOE 227	0.08	3	6.818	6.929	2%
	0.1	3	8.514	8.233	3%
	0.12	3	10.206	9.402	8%

Above Table 4.8 shows the comparison between CFD and theory for all the six blade designs. It also shows that the accuracy of theoretical prediction is more than 90%.

CHAPTER 5: RESULTS AND DISCUSSION

5.1 Result Analysis

From our CFD experiments, we saw that the number of blades, chord length, and airfoil shape greatly impact torque and thrust of the blade. In this section, we will graphically describe these parameters.

First Three Cases,

Airfoil : NACA 2410

Chord : 0.1 m

Blade Number : 2, 3, and 6

Thrust Study :

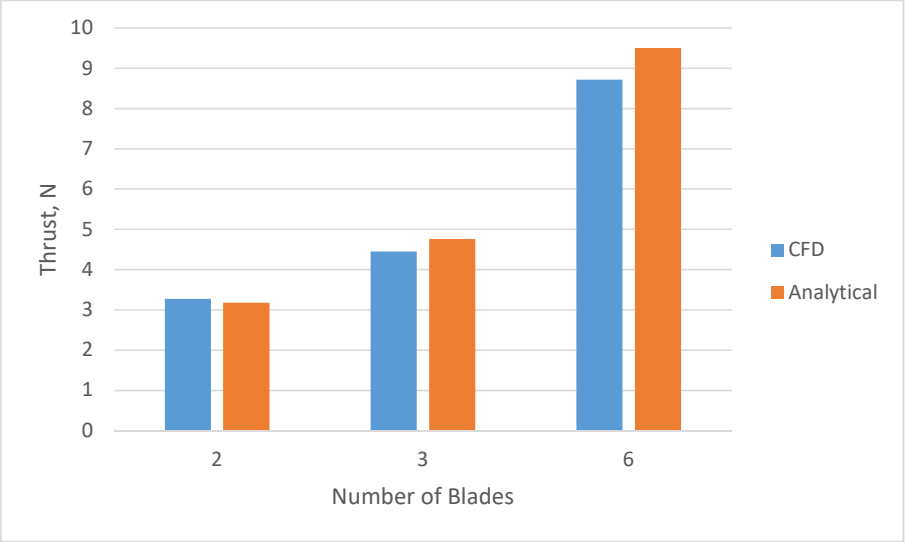

Figure 5.1: Thrust vs. Number of Blades

In the above graph the relation between thrust and number of blade of NACA 2410 aerofoil is shown both computationally (CFD) and theoretically. The blue bars are representing CFD values for thrust and orange bars are representing theoretical values for thrust. From the graph it is visible that our theoretical model can predict more than 90% accurate result.

Torque Study :

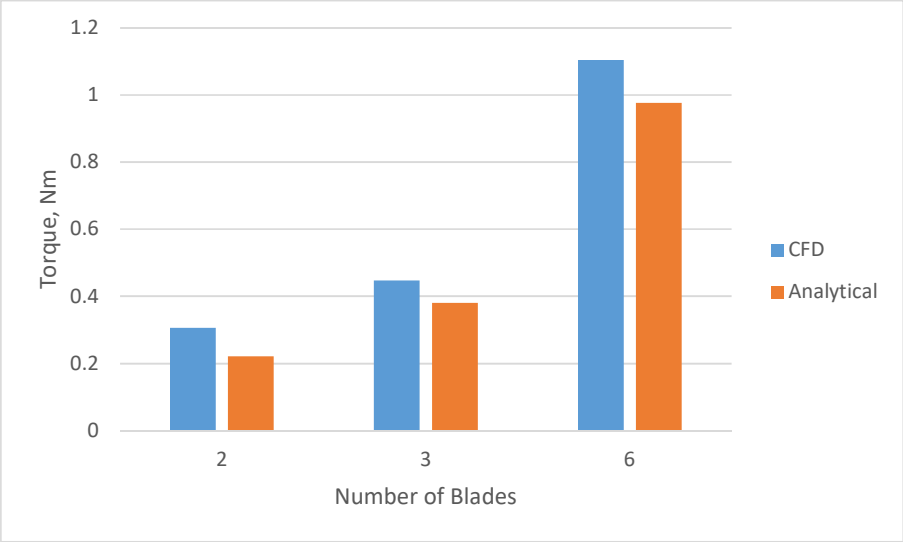

Figure 5.2: Torque vs. Number of Blades

In the above graph the relation between torque and number of blade of NACA 2410 aerofoil is shown both computationally (CFD) and theoretically. The blue bars are representing CFD values for torque and orange bars are representing theoretical values for torque. From the graph it is visible that our theoretical model can predict more than 85% accurate result.

Last Three Cases,

Airfoil : GOE 227

Chord : 0.08 m, 0.1m, and 0.12m

Blade Number : 3

Thrust Study :

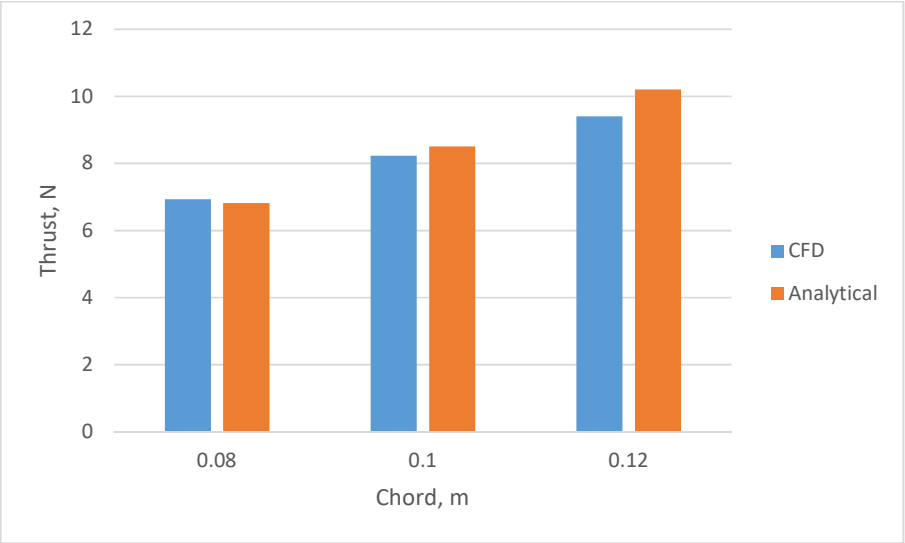

Figure 5.3: Thrust vs. Chord

In the above graph the relation between thrust and number of blade of GOE 227 aerofoil is shown both computationally (CFD) and theoretically. The blue bars are representing CFD values for thrust and orange bars are representing theoretical values for thrust. From the graph it is visible that our theoretical model can predict more than 90% accurate result.

Torque Study :

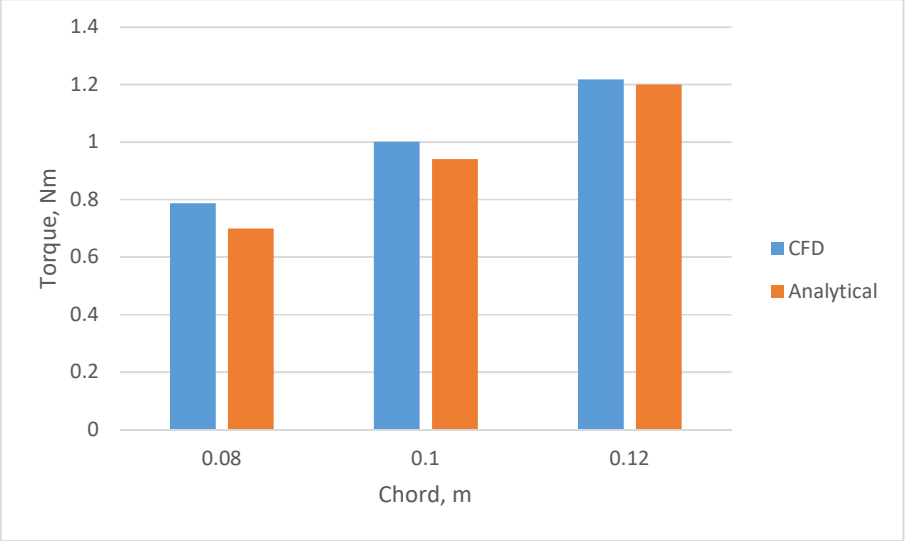

Figure 5.4: Torque vs. Chord

In the above graph the relation between torque and number of blade of GOE 227 airfoil is shown both computationally (CFD) and theoretically. The blue bars are representing CFD values for torque and orange bars are representing theoretical values for torque.

From the graph it is visible that our theoretical model can predict more than 85% accurate result.

5.2 Comparison with Traditional Ceiling Fan

In this section, we compare the traditional fan (300 rpm) axial velocity at 1.5 m below the fan to our new modified design with the parameters below.

Airfoil	: GOE 227
Chord	: 0.08 m
Number of Blades	: 3
Angular Velocity	: 200 rpm

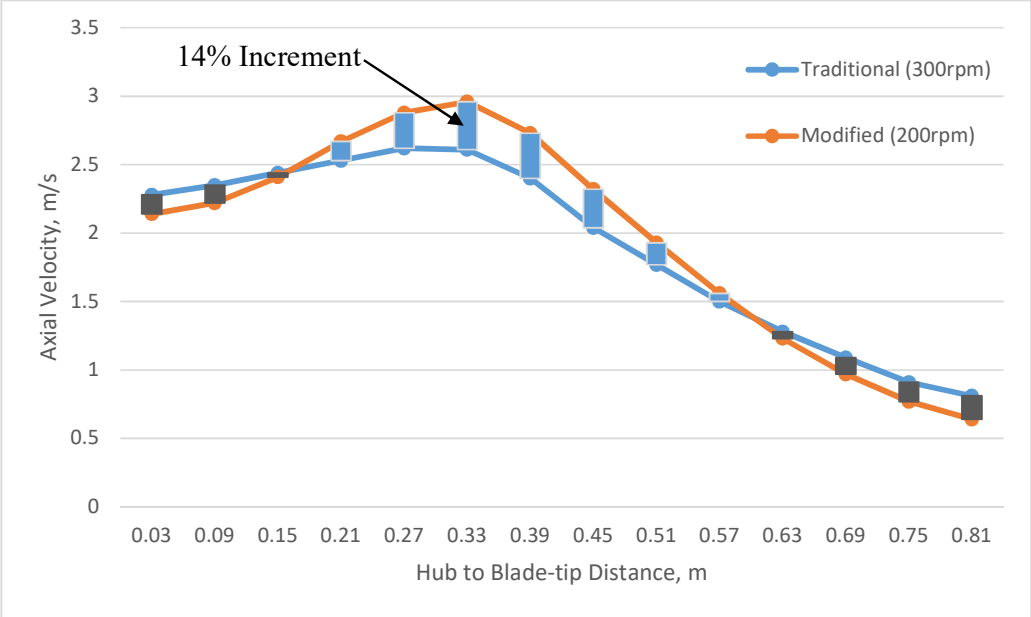

Figure 5.5: Axial Velocity at 1.5 m from Fan Blade

The blue line represents axial velocity of traditional fan blade at 1.5 m below the fan and the orange line represents new designed blade using GOE 227 airfoil. The peak velocity of newly designed fan is 14% more than traditional fan and operates at 200 rpm whether traditional fan operates at 300 rpm.

Efficiency Calculation:

Table 5.1: Comparing Efficiency between Traditional and Modified Fan Blade

Fan Type	Axial Velocity at Blade (m/s)	Angular Velocity (rpm)	Torque (Nm)	Thrust (N)	Power Input (W)	Power Output (W)	Efficiency
Traditional	1.3	300	0.656	6.137	20.61	7.9781	38%
Modified	1.44	200	0.7873	6.929	16.49	9.9777	60%

5.3 Discussion

From the above graph and table, we can deduce that our modified fan blade has a 14% higher peak axial velocity at 1.5 m below the fan and a 22% improved power efficiency.

CHAPTER 6: CONCLUSION AND RECOMMENDATIONS

6.1 Conclusion

This paper focused on developing a new theoretical model for designing more efficient ceiling fan blades. These mathematical equations are derived from the basic theories of aerodynamics e.g. Momentum Theory, Blade Element Theory, Lifting Line Theory, and the conservation laws of fluid dynamics e.g. Conservation of Mass, Momentum, and Energy. Some assumptions are made to simplify the problem. The validity of these equations was checked by using Numerical Methods such as CFD, the results from the numerical solutions give promising results. These equations can predict more than 90% accurate results when compared with numerical solutions. Blades designed using these equations deliver 14% more axial velocity at 1.5 m below the fan and consume 22% less energy to run.

6.2 Recommendations

- Performing experiment and providing experimental data might add more validity to the study.
- Adding variability to the chord of the blade may improve energy efficiency even further.

REFERENCES

1. Jain, A., Upadhyay, R., Chandra, S., Saini, M. K., & Kale, S. (2004). Experimental Investigation of the Flow Field of a Ceiling Fan. 2004 ASME Heat Transfer/Fluids Engineering Summer Conference. https://doi.org/10.1115/ht-fed2004-56226
2. Schmidt, K. & Patterson, D. J. (2001). Performance results for a high-efficiency tropical ceiling fan and comparisons with conventional fans: Demand side management via small appliance efficiency. Renewable Energy, 22, pp. 169–176.
3. Dhurvey, P., Kumar Pathak, N., Soni, S., and Pandey, A. (2018). Aerodynamic and Structural Analysis of Ceiling Fan for Different Blade Materials. Materials Today: Proceedings, 5(9), pp. 19604-19613. https://doi.org/10.1016/j.matpr.2018.06.323
4. Mahlia1, T. M. I., Moradalizadeh, H., et al. (2011). Theoretical and Experimental Investigation of Energy Efficiency Improvement of the Ceiling Fan by Using Aerodynamic Blade Profile. Journal of Energy & Environment, 3(01), pp. 40-49.
5. Rajapakshe, P. D. M. P., Mapa, M. H. H. G. et al. (2015). Investigating Aerodynamic Performance of a Ceiling Fan. Annual Sessions of IESL, The Institution of Engineers, Sri Lanka, pp.1– 10.
6. Afaq, M. A., Maqsood, A., et al. (2017). Aerodynamic investigation and redesign of ceiling fan blades for enhanced energy efficiency. Maejo Int. J. Sci. Technol., 11(02), pp. 97-114.
7. Ahmed, J. U., Uddin, M. J., Farnaz, N., & Ali, M. (2016). National Fans Limited of Bangladesh. Asian Case Research Journal, 20(02), 351–372. https://doi.org/10.1142/s0218927516500139
8. NASA Glenn Research Center. (2022, July 21). *What is Lift? | Glenn Research Center | NASA*. Glenn Research Center | NASA. https://www1.grc.nasa.gov/beginners-guide-to-aeronautics/what-is-lift
9. Sheng, R. (2019). Systems engineering fundamentals. In *Elsevier eBooks* (pp. 113–206). https://doi.org/10.1016/b978-0-12-816458-7.00007-7

10. Froude, William (1865, April 6). On the Mechanical Principals of the Action of Propellers. Transactions of the Royal Institution of Naval Architects, 6: 13 – via Hathi Trust.
11. Froude, Robert (1889, April 12). On the Part Played in Propulsion by Differences in Fluid Pressure. Transactions of the Royal Institution of Naval Architects, 30: 390 – via Hathi Trust.2.
12. Froude, William (1878, April 11). The Elementary Relation between Pitch, Slip, and Propulsive Efficiency. Inst. Naval Architects, 19: 47 – via Hathi Trust.
13. Anderson, J. D., Jr. (2016). Fundamentals of Aerodynamics. McGraw-Hill Education.
14. Versteeg, H. K., & Malalasekera, W. (2007). An introduction to computational fluid dynamics. Pearson Education Limited, 2, pp. 186-211.
15. Marine propellers and propulsion. (2012). In *Elsevier eBooks*. https://doi.org/10.1016/c2010-0-68327-1

APPENDIX

NACA 2410

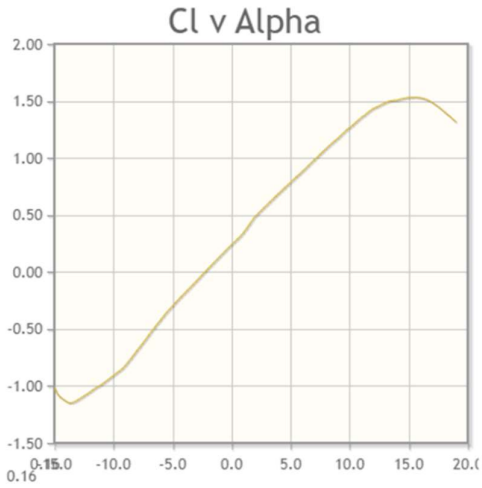

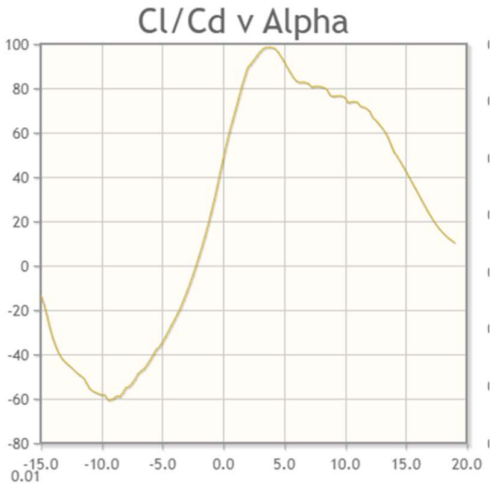

GOE 227

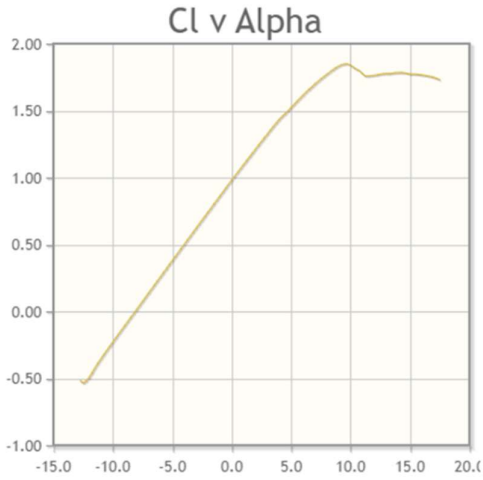

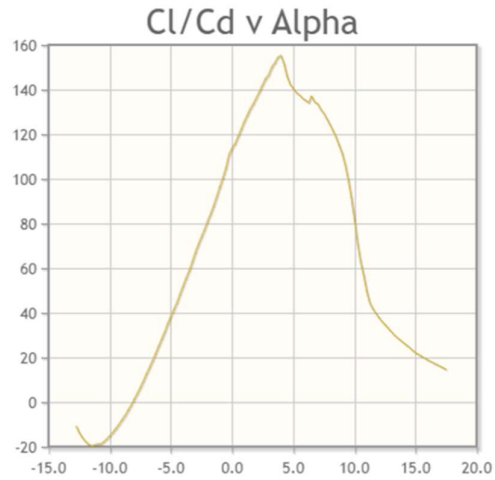

Induced Drag Factor